

Comparative morphology of the musculature of the sting apparatus in *Ampulex compressa* (Hymenoptera, Ampulicidae) and *Sceliphron destillatorium* (Hymenoptera, Sphecidae)

Stefan Graf^{1,2}, Maraike Willsch¹, Michael Ohl¹

¹ Museum für Naturkunde Berlin, Invalidenstraße 43, 10115 Berlin, Germany

² Humboldt Universität zu Berlin, Unter den Linden 6, 10117 Berlin, Germany

<http://zoobank.org/98A7ABB2-3264-46C6-AF34-A2E5EE9CCE9A>

Corresponding author: Stefan Graf (stefan.graf@mf.n.berlin)

Academic editor: D. Zimmermann ♦ Received 2 September 2020 ♦ Accepted 24 November 2020 ♦ Published 5 January 2021

Abstract

The sting apparatus of aculeate Hymenoptera is derived from the ovipositor and is their most prominent apomorphy. In contrast to the frequently analysed sclerites of the sting apparatus, the associated musculature has largely been neglected. In this study, we use micro-computed tomography to present a detailed description of the musculature of the sting apparatus of *Ampulex compressa* (Ampulicidae) and *Sceliphron destillatorium* (Sphecidae). We found that 12 of 15 muscles corresponding to the sting apparatus are homologous between both species examined and 13 muscles in comparison with Hymenoptera described in the literature. All muscles identified as critical for the act of stinging were found in both species. Moreover, we found the ventral tergum 8–tergum 9 muscle and the tergum 8–tergum 8 muscles in *A. compressa* and the second valvifer–second valvifer muscle in *S. destillatorium*. For the first time, we describe the ventral tergum 8–tergum 9 muscle and the second valvifer–second valvifer muscle that interconnects both body sides, in Hymenoptera.

Key Words

abdomen, Aculeata, anatomy, microCT, stinger

Introduction

With over 150,000 described species, Hymenoptera is one of the largest insect orders (Aguiar et al. 2013). Approximately 70,000 of the species belong to the sub-clade Aculeata (Grimaldi and Engel 2005). The name-giving apomorphic character of the Aculeata (aculeatus: Latin for sharp, spiny) is the sting apparatus that evolved from the ovipositor (Smith 1970, Sharkey et al. 2012). The monophyletic Aculeata are divided into three superfamilies: Apoidea, Chrysidoidea, and Vespoidea (Aguiar et al. 1992, Branstetter et al. 2017). Apoidea comprises the monophyletic Anthophila (bees) and the paraphyletic “apoid wasps”, Sphecidae in the broad sense, or “digger wasps” (Ohl and Engel 2007, Branstetter et al. 2017).

Currently, about 10,000 species of apoid wasps are known (Pulawski 2020). Historically, they are divided

into Crabronidae, Ampulicidae, Sphecidae, and Heterogynaidae (Branstetter et al. 2017). Recent studies suggest Ammoplanina to be the sister-group of Anthophila (Sann et al. 2018). While Sphecidae and Ampulicidae are thought to be well supported clades (Ohl and Spahn 2010, Peters et al. 2017, Sann et al. 2018), the monophyly of Crabronidae (Ohl and Bleidorn 2006, Lohrmann et al. 2008, Ohl and Spahn 2010, Peters et al. 2017) is questioned in several studies (e.g. Lohrmann et al. 2008, Sann et al. 2018). Heterogynaidae are found nested within Bembicinae by Sann et al. (2018), while Branstetter et al. (2017) suggested Heterogynaidae to be the sister-group to a paraphyletic grouping of Crabroninae and Sphecidae. Furthermore, Sann et al. (2018) suggested Ammoplanidae, Psenidae, Pemphredonidae, Philantidae, Bembicidae, Crabronidae, Mellinidae, Sphecidae, Astatidae and Ampulicidae to be monophyletic taxa.

Morphological studies are important sources for phylogenetic analyses (e.g. Ohl and Spahn 2010, Vilhelmsen et al. 2010, Da Silva et al. 2014, Zimmermann and Vilhelmsen 2016, Liu et al. 2019, Willsch et al. 2020, Barbosa et al. 2021). Much has been written about the sclerites of the sting apparatus of Aculeata (e.g. Snodgrass 1933, Trojan 1935, Rietschel 1937, Kugler 1978, Hermann and Chao 2002, Packer 2003), including apoid wasps (Matushkina 2011, Mosel 2014, Gadallah and Assery 2015, Matushkina and Stetsun 2016). Apart from older studies (Snodgrass 1933, Trojan 1935, Rietschel 1937), examination of the musculature of the sting apparatus has been largely neglected. More recently, Kumpanenko and Gladun (2018) published a study on the musculature and sclerites of the sting apparatus of *Cryptocheilus versicolor* (Pompilidae). Barbosa et al. (2021) published the latest work on the sting apparatus of Chrysidoidea, which is the most basal taxon of Aculeata. Both recent publications of Kumpanenko and Gladun (2018) and Barbosa et al. (2021) do not describe the musculature connecting the sting apparatus to the cuticle, though.

We present a comparative description of the musculature of two representatives of apoid wasps: *Ampulex compressa* (Fabricius, 1781) (Ampulicidae) and *Sceliphron destillatorium* (Illiger, 1807) (Sphecidae). Apoid wasps use their stinger primarily as a tool for hunting prey for the offspring (Grimaldi and Engel 2005). The adult female is usually a solitary, vegetarian flower visitor, while the larvae feed on paralysed arthropods deposited in the nest (Grimaldi and Engel 2005, Ohl and Engel 2007). *S. destillatorium* builds a mud nest and provides multiple cells with paralysed spiders (Fateryga and Kovblyuk 2014). The spiders are carried with the mandibles (Evans 1962). After provisioning, the cells are sealed with mud and either additional cells or a new nest is constructed (Bohart and Menke 1976, Fateryga and Kovblyuk 2014). *A. compressa* preys upon cockroaches and its unusual stinging behaviour is well documented (Haspel et al. 2003, Libersat 2003, Catania 2018): The adult female grasps the lateral margin of the cockroach's pronotum, then bends her metasoma downwards to sting the cockroach for paralyzing. Two stings accurately hit the ganglions in the head and thorax. The venom inhibits the escape behaviour of the cockroach while the locomotion remains unaffected (Libersat 2003). This allows *A. compressa* to lead her prey into the nest by grasping one antenna. A single egg is laid on the cockroach before the wasp finally seals the nest entrance with substrate (Bohart and Menke 1976, Haspel et al. 2003, Libersat 2003, Catania 2018).

The aim of this study is to provide detailed morphological descriptions of the sting apparatus in order to contribute to the understanding of morphological adaptations and the phylogeny of the paraphyletic apoid wasps. *A. compressa* and *S. destillatorium* were chosen as otherwise well-studied species within the apoid wasps (see above), with a high number of plesiomorphic characters (Ohl and Spahn 2010) and a basal position within the Apoidea (Branstetter et al. 2017, Sann et al. 2018).

In addition to evaluating the phylogenetic significance of morphological characters, this study discusses functional aspects of the sting apparatus in apoid wasps.

Methods

Specimens examined

We compared the musculature of the sting apparatus of the females of *A. compressa* (Ampulicidae) and *S. destillatorium* (Sphecidae). Muscles directly connected to the sting apparatus were described. The specimens belong to the Hymenoptera collection of the Museum für Naturkunde Berlin (MfN). In addition to the μ CT scans of one specimen per species, dissections of four additional specimens of *A. compressa* and three additional specimens of *S. destillatorium* were conducted to confirm the spatial position and shape of the sclerites and muscles. See Suppl. material 1: Table S1 for a detailed list of specimens and their collection/rearing data.

3D imaging

The specimens used for 3D imaging were stored in 96% ethanol. They were stained with 25% iodine in pure ethanol (100%), to improve contrast in μ CT scans (Metscher 2009, Gignac et al. 2016, Willsch et al. 2020). Before staining, the extremities and the anterior half of the thorax were removed to avoid obstructions during the scan and to ensure a uniform staining result. After three days of staining, the specimens were washed in 100% ethanol for 30 seconds to remove excess iodine. To prevent fissures and ripped muscles, the specimens were dried carefully using a critical point dryer (Leica EM CPD300).

The specimens were imaged using a μ CT (Phoenix nanotom X-ray | s) at 50 kV and 150 μ A. 1440 images per scan were taken, each with an exposure time of 1 second. For *S. destillatorium*, a resolution of 4 μ m/pixel was achieved. The resolution for *A. compressa* was set at 3.6 μ m/pixel. The size of the specimens required a multi-scan consisting of three single scans. The stacking and the cone beam reconstruction was accomplished with the software PHOENIX | X-RAY DATOS | X 2.0 (GE Sensing & Inspection Technologies GmbH). We manually segmented the musculature and sclerites using AMIRA ZIB Edition 6.4.0 and former versions (provided by the Zuse Institute Berlin). Only the left body side was segmented, based on the bilateral symmetry.

Dissections

The dissected specimens were preserved in 96% or 70% ethanol. The dissections were conducted under a Leica S8APO Binocular with forceps, scissors and preparation needles. The gaster was opened by destructive removal

of the fourth abdominal segment. Consecutive terga and sterna could easily be removed as a whole with forceps. Only the seventh tergite and sternite had to be removed with great care, to not rip the muscles of T8. Once the sting apparatus was exposed, muscles and sclerites were removed one by one from the outside, or scissors were used to cut a sclerite with all muscles loose from the rest of the sting apparatus.

The illustrations were drawn in Adobe Illustrator CS5 and labelled as well as resized in Photoshop CS5. The remaining sclerites are stored in separate tubes with the specimens in the alcohol collection of the MfN.

Terminology

Based on Vilhelmsen (2000a, b), Vilhelmsen et al. (2001) and the Hymenoptera Anatomy Ontology (HAO, Yoder et al. 2010, <http://portal.hymao.org/projects/32/public/ontology/>), muscle terminology is composed of the points of origin and insertion. The fan-like part of a muscle is the origin, whereas the tendon is located at the insertion. If possible, the insertion and origin of muscles already described in the literature were adopted to ensure comparability, e.g. when the muscle has tendons on both ends. To differentiate muscles with origin or insertion on the same sclerites, suffixes (for abbreviations see below) are used (summed up in Mikó et al. 2007). Sclerite terminology is based on the HAO and Vilhelmsen (2001). The names of muscles were adopted from the HAO if possible; new names were assigned according to the HAO conventions, if necessary. Comparisons to illustrations by Kumpanenko and Gladun (2018, fig. 6c) as well as Matushkina (2011, fig. 1A) confirm that the scanned *S. destillatorium* was preserved with an extended stinger. To maintain comparability between both specimens, the following descriptions of muscle insertions and origins assume the positions of the sclerites with retracted stinger in *S. destillatorium*. The abbreviations used are the following:

Sclerites:

1vf	first valvifer;
2vf	second valvifer;
(1–3) vv	first to third valvula, respectively;
fu	furcula;
1r	first ramus;
2r	second ramus;
T8	tergum 8;
T9	tergum 9;
T7	abdominal tergum 7;
S7	abdominal sternum 7;
sp	spiracle;
spa	sensillar patch.

Suffixes:

d	dorsal;
----------	---------

v	ventral;
l	lateral;
m	medial;
a	anterior;
p	posterior.

Results

The metasomal apex

In *A. compressa*, the metasoma is laterally compressed and acuminate. Both the ventral and dorsal metasomal margins are bent towards the tip in a nearly identical way. The dorsal margin of the metasomal apex in *S. destillatorium* is straight and the ventral metasomal margin bends up towards the tip with the first, second and third valvulae. The stinger is noticeably farther extended in our scan of *S. destillatorium*, compared to *A. compressa* (Fig. 1).

Sclerites

Dissections under the binocular confirm that the sting apparatus of both species consists of the same skeletal structures with similar spatial relation as in previously studied Hymenoptera: T8 and T9, a pair of first and second valvifers with their respective first and second rami, the furcula, the first and two second valvulae forming the sting and a pair of third valvulae (Rietschel 1937, Kugler 1978, Matushkina 2011, Da Silva et al. 2014, Mosel 2014, Kumpanenko and Gladun 2018) (Fig. 1). T8 of *A. compressa* is arch-shaped and nearly rectangular in lateral view. The arch is sclerotised anteriorly and consists of a round, membranous area posteriorly; left and right half of T8, delimiting the membranous area, do not connect posteriorly (Fig. 1A). In contrast, the sclerotised parts of T8 of *S. destillatorium* show a complex, question mark-like shape in lateral view, the sclerotised dorsal arch is thin. A membranous area, limited posteriorly by a lightly sclerotised arch, gives T8 of *S. destillatorium* an outline similar to T8 of *A. compressa* (Fig. 1B, the posterior arch is indicated by a single yellow outline). In both species T8 forms a lateral lamella ventrally, which muscles attach to. The T9 of *S. destillatorium* shows a heavily sclerotised, dorsal anal arch with anterodorsal apodems on each side that connects the oval halves of the sclerite (Fig. 1B). In *A. compressa* the anal arch is thin and positioned on the anterior edge of T9, thereby not overarching the second valvifer. The second valvifers bear strong interspecific differences (Figs 1, 5). In *A. compressa* the second valvifer is roughly triangular with the dorsal and ventral edge connecting posteriorly without a conspicuous posterior edge. In *S. destillatorium* the second valvifer is approximately trapezoidal, with an anterior edge between dorsal and ventral edge. The third valvula is not connected to the posterior edge. The articular process of the second valvifer is very pronounced and elongate.

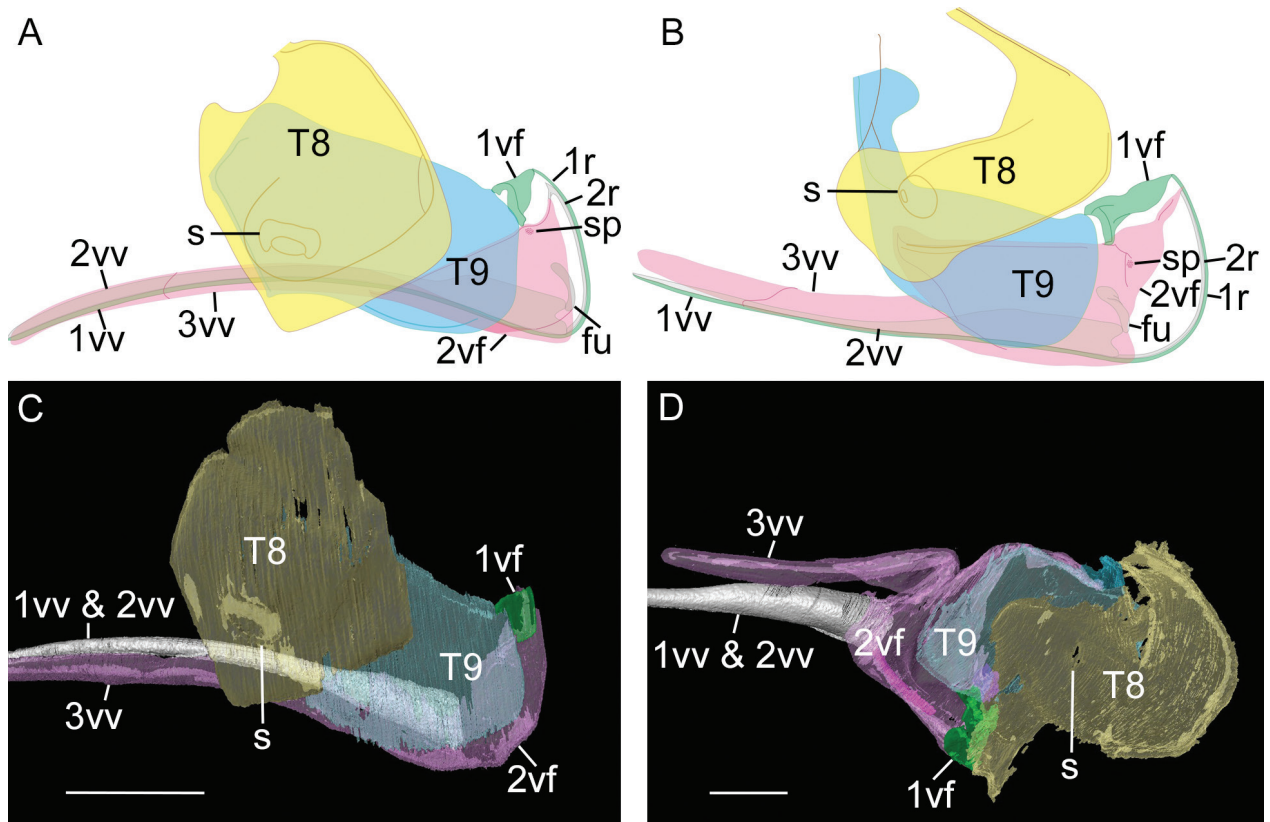


Figure 1. Overview of the sclerites of the sting apparatus. Lateral view, anterior to the right. **A.** *Ampulex compressa*, line drawing from dissections; **B.** *Sceliphron destillatorium*, line drawing from dissections; **C.** *Ampulex compressa*, 3D reconstruction; **D.** *Sceliphron destillatorium*, 3D reconstruction, stinger extended. **1vv** – first valvula; **2vv** – second valvula; **3vv** – third valvula; **fu** – furcula; **r1** – first ramus; **r2** – second ramus; **1vf** – first valvifer; **2vf** – second valvifer; **T9** – tergum 9; **T8** – tergum 8; **sp** – spiracle; **spa** – sensillar patch. Scale bars: 0.5 mm.

Both species possess sensillar patches on the second valvifer (Vilhelmsen 2001c, Matushkina 2011), ventral to the first valvifer-second valvifer articulation. The first valvifer are of comparable form, with a convex and heavily sclerotised posterior edge between the dorsal articulation to T9 and the ventral articulation to the second valvifer. It is longer, stretched anteriorly, in *S. destillatorium*. Mosel (2014) provides detailed descriptions and illustrations of the sclerites of *A. compressa*.

The position of the sclerites differs among the specimens in our scans (Fig. 1D). In *S. destillatorium*, the second valvifer, T9, and the first valvifer are rotated roughly 90° posteroventrally in relation to the stinger and the T8. The second valvifer and T9 maintain their relative position to each other. The first valvifer, articulating to the T9, is located ventrally in *S. destillatorium* and dorsally in *A. compressa*. The third valvula of *S. destillatorium* is bent ventrally in a sharp angle from the second valvifer and the stinger is extended far beyond the apex of the metasoma (Fig. 1C, D).

Muscles

We found 15 muscles (Table 1) that interconnect the sclerites of the sting apparatus or connect the sting apparatus

as a whole to the cuticle. Fourteen of them appear in *A. compressa* and 13 in *S. destillatorium*. There are 12 muscles homologous between both species. In the following, the musculature of *A. compressa* is described in detail. Additional and differing muscles of *S. destillatorium* are specified subsequently.

Ampulex compressa

Abdominal tergum and abdominal sternum 7 to tergum 8 (Fig. 2A)

Dorsal tergum 7-tergum 8 muscle (dT7-T8) arises anteriorly on the apodeme of T7 and inserts ventrally on the sclerotised arch between both halves of T8. **Ventral tergum 7-tergum 8 muscle (vT7-T8)** arises on the apodeme of T7 and inserts on the anterior edge of the T8, ventral of dT7-T8. The muscle is not bipartite in *A. compressa*. **Posterior tergum 7-tergum 8 muscle (pT7-T8)** arises anterodorsally on T7 and inserts close to the anterior edge of T8, dorsal of the lateral lamella, where T8 is most sclerotised. **Sternum 7-tergum 8 muscle (S7-T8)** arises anteriorly on the apodeme of S7 and inserts anteroventral on the medial flank of the lateral lamella of T8.

Table 1. Muscles with origin and insertion. 1 = muscle present, 0 = muscle absent.

Abbr.	Name	Origin	Insertion	<i>Ampulex compressa</i>	<i>Sceliphron destillatorium</i>
abdominal tergum and abdominal sternum 7 to tergum 8					
dT7-T8	dorsal tergum 7-tergum 8 muscle [†]	anterior, apodeme of T7	dorsal sclerotised arch between both sides of T8	1	1
pT7-T8	posterior tergum 7-tergum 8 muscle [†]	posterior on T7	anteroventral near the heavily sclerotised edge of T8	1	1
vT7-T8 a	ventral tergum 7-tergum 8 muscle a [†]	apodeme of T7	anterior edge of T8	1	1
vT7-T8 b	ventral tergum 7-tergum 8 muscle b [†]	apodeme of T7	anterior edge of T8, ventral of vT7-T8 a	muscle not divided into two portions	1
S7-T8	tergum 8-sternum 7 muscle [†]	anterior, apodeme of S7	anteroventral, medial flank on the lateral lamella of T8	1	1
tergum 8 to tergum 9 and first valvifer					
dT8-T9	dorsal tergum 8-tergum 9 muscle	anterodorsal on the medial flank of T8	posterodorsal on or near the anal arch of T9	1	1
lT8-T9	lateral tergum 8-tergum 9 muscle	medial flank of T8, dorsal of dT8-T9	dorsal or central on the lateral flank of T9	1	1
T8-1vf	tergum 8-first valvifer muscle	posteromedial on the lateral lamella of T8	posterior edge of 1vf	1	1
T8-T8	tergum 8-tergum 8 muscle [†]	medial flank of T8, along the anterior edge	anteroventral of the spiracle	1	0
vT8-T9	ventral tergum 8-tergum 9 muscle [‡]	anteroventral, medial flank of T8	central, lateral flank of T9	1	0
tergum 9 to second valvifer					
dT9-2vf a	dorsal tergum 9-second valvifer muscle a	laterodorsal flank of T9	posterior edge of articular process	1	1
dT9-2vf b	dorsal tergum 9-second valvifer muscle b	mediodorsal flank of T9	posterior edge of articular process	1	1
vT9-2vf	ventral tergum 9-second valvifer muscle	anteromedial flank of T9, along the anterior edge	posterior, lateral flank of the second valvifer	1	1
pT9-2vf	posterior tergum 9-second valvifer muscle	ventral of the anal arch of T9	posterodorsal on the second valvifer	1	1
second valvifer to furcular					
2vf-2vf	second valvifer-second valvifer muscle [†]	dorsal, anteromedial flank of second valvifer	equivalent point of insert on opposing second valvifer	0	1
l2vf-fu	lateral second valvifer-furcula muscle [†]	anteroventral, medial flank of the second valvifer	dorsal arm of the furcula	1	1
m2vf-fu	medial second valvifer-furcula muscle [†]	posteroventral, medial flank of the second valvifer	lateral arm of the furcula	1	1

† = newly named in HAO scheme ‡ = newly identified.

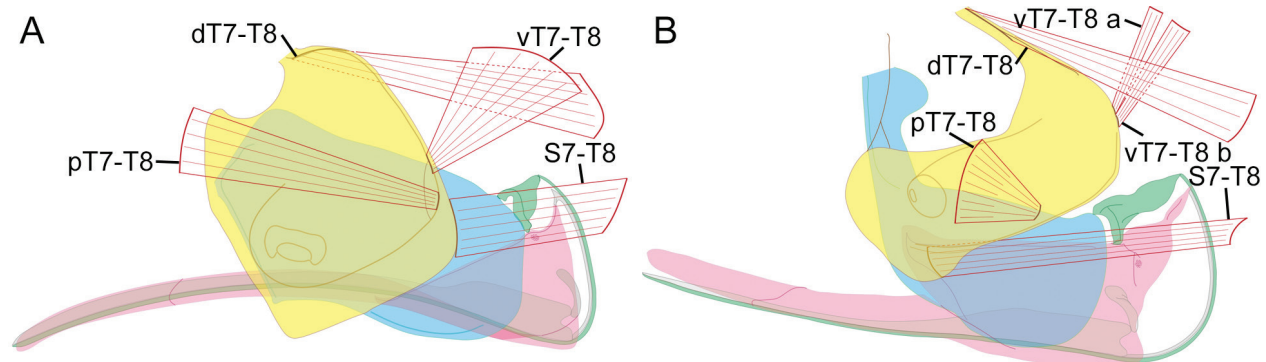


Figure 2. The musculature connecting T8 to the cuticula. Lateral view, anterior to the right, line drawing from dissections. **A.** *Ampulex compressa*; **B.** *Sceliphron destillatorium*. **dT7-T8** – dorsal tergum 7-tergum 8 muscle; **vT7-T8 (a & b)** – ventral tergum 7-tergum 8 muscle (portion a and b respectively); **pT7-T8** – posterior tergum 7-tergum 8 muscle; **S7-T8** – sternum 7-T8 muscle.

Tergum 8 (Fig. 3A)

Tergum 8-tergum 8 muscle (T8-T8) arises on the medial flank near the anterior edge of T8 and inserts on the ventral medial flank of T8 posteroventral on the sclerotised rim of the spiracle.

Tergum 8 to tergum 9 and first valvifer (Fig. 3A)

Dorsal tergum 8-tergum 9 muscle (dT8-T9) arises on the medial flank along the anterodorsal edge of T8 and inserts

laterally on the posterior edge of T9, dorsal of the anal arch (Fig. 3D). **Lateral tergum 8-tergum 9 muscle (lT8-T9)** arises dorsally, along the connection of both halves of T8 on the medial flank, dorsal of dT8-T9. It inserts centrally on the lateral flank of T9. The dT8-T9 and lT8-T9 arise close together and run in a roughly perpendicular angle from each other. The **tergum 8-first valvifer muscle (T8-1vf)** arises anteriorly on the lateral lamella of T8 and inserts on the posterior edge of the first valvifer, close to the articulation to T9. **Ventral tergum 8-tergum 9 muscle (vT8-T9)** arises anteroventrally on the medial flank of T8

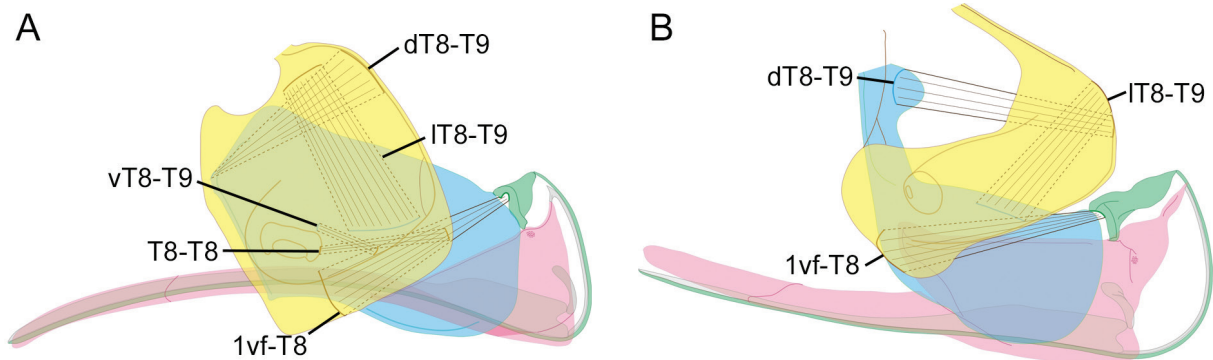


Figure 3. The musculature interconnecting T8 and T9. Lateral view, anterior to the right, line drawing from dissections. **A.** *Ampulex compressa*; **B.** *Sceliphron destillatorium*. **dT8-T9** – dorsal tergum 8-tergum 9 muscle; **IT8-T9** – lateral tergum 8-tergum 9 muscle; **T8-1vf** – T8-1vf muscle; **T8-T8** – tergum 8-tergum 8 muscle; **vT8-T9** – ventral tergum 8-tergum 9 muscle.

and inserts centrally on the lateral flank of T9, near the posteroventral edge. The muscle is small and rod-like.

Tergum 9 to second valvifer (Fig. 4A)

Dorsal tergum 9-second valvifer muscle a (dT9-2vf a) arises from the lateral flank of T9, dorsal of the anal arc. The muscle inserts at the posterior edge of the articular process of the second valvifer. **Dorsal tergum 9-second valvifer muscle b (dT9-2vf b)** arises posterodorsally from the medial flank of T9 anterior of the anal arch. It inserts on the posterior edge of the articular process of the second valvifer, ventral to **dT9-2vf a**. The anal arch of T9 is not heavily sclerotised, thus **dT9-2vf a** and **b** arise on the flank of the sclerite. They run parallel and only differ in their origin on the medial or lateral flank of T9. **Ventral tergum 9-second valvifer muscle (vT9-2vf)** arises from the medial flank of T9 along the anterior and ventral edge, inserts laterally along the very short posterior edge of the second valvifer. **Posterior tergum 9-second valvifer muscle (pT9-2vf)** arises anteroventrally on the anal arch and inserts posteriorly on the dorsal edge of the second valvifer, close to **m2vf-fu** and **vT9-2vf**.

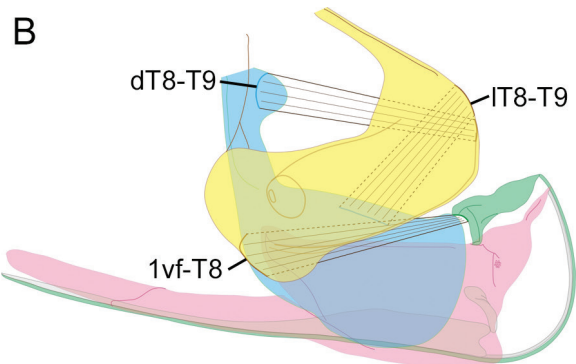
Second valvifer to furcula (Fig. 5A)

Lateral second valvifer-furcula muscle (l2vf-fu) arises anteroventrally on the medial flank of the second valvifer, runs lateral of **m2vf-fu** and inserts on the dorsal arm of the furcula. **Medial second valvifer-furcula muscle (m2vf-fu)** arises posteroventrally on the second valvifer, close to **m2vf-fu** and **vT9-2vf**, runs medial of **l2vf-fu** and inserts on the lateral arm of the furcula.

Sceliphron destillatorium

Abdominal tergum and abdominal sternum 7 to tergum 8 (Fig. 2B)

Dorsal tergum 7-tergum 8 muscle (dT7-T8) arises on the anterior apodeme of T7 and inserts dorsally on the



sclerotised arch between both halves of T8. **Ventral tergum 7-tergum 8 muscle a (vT7-T8 a)** arises on the apodeme of T7 and inserts dorsal on the anterior edge of T8, ventral of **dT7-T8**. **Posterior tergum 7-tergum 8 muscle (pT7-T8)** arises anterodorsally on T7 and inserts close to the ventral edge of T8, anterodorsal of the lateral lamella, close to the sclerotised edge. **Ventral tergum 7-tergum 8 muscle b (vT7-T8 b)** arises on the apodeme of T7 and inserts dorsally on the anterior edge of T8, ventral to the insert of **vT7-T8 a**.

Tergum 8 to tergum 9 and first valvifer (Fig. 3B)

Dorsal tergum 8-tergum 9 muscle (dT8-T9) arises on the medial flank along the anterior edge of T8 and inserts laterodorsally the apodeme of the anal ark of T9 (Fig. 3C). **Lateral tergum 8-tergum 9 muscle (IT8-T9)** arises near the anterior edge of the T8, on the medial flank, dorsal of **dT8-T9**. It inserts on the lateral flank of T9 along the dorsal edge. **Tergum 8-first valvifer muscle (T8-1vf)** arises medially on the posteroventral flank near the edge of the lateral lamella of T8 and inserts on the posterior edge of the first valvifer, close to the articulation to T9.

Tergum 9 to second valvifer (Fig. 4B)

Dorsal tergum 9-second valvifer muscle a (dT9-2vf a) arises from the anterior edge of the anal arch, ventral of the apodeme. It inserts at the posterior edge of the articular process of the second valvifer. **Dorsal tergum 9-second valvifer muscle b (dT9-2vf b)** arises from the medial flank of the anal arch of T9, near the posterior margin, ventral of **dT9-2vf a**. It inserts at the posterior edge of the articular process of the second valvifer, ventral to **dT9-2vf a**. In *S. destillatorium*, the anal arch is heavily sclerotised (compare Fig. 1B, D with figs 2b, 5b in Kumpanenko and Gladun 2018). **Posterior tergum 9-second valvifer muscle (pT9-2vf)** arises posteriorly on the ventral edge of the anal arch of tergum 9 and inserts posteriorly on the dorsal edge of the second valvifer, close to **m2vf-fu** and **vT9-2vf**.

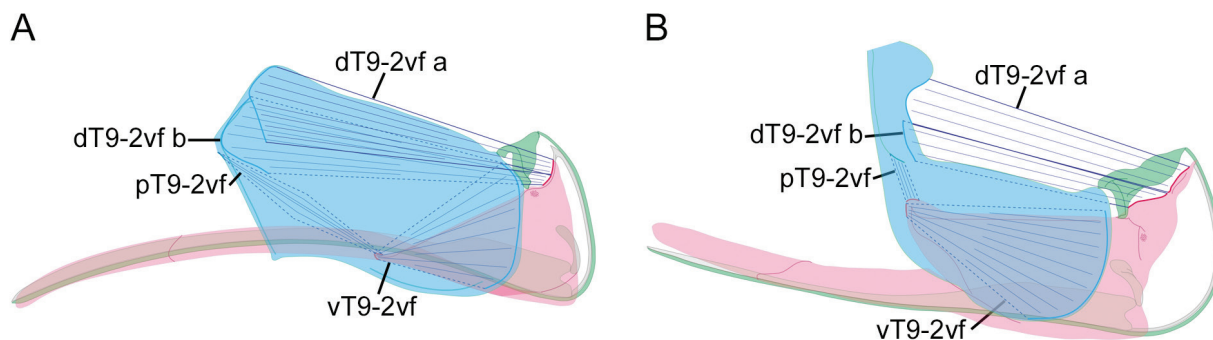


Figure 4. The musculature interconnecting T9 and the second valvifer. Lateral view, anterior to the right, line drawing from dissections. **A.** *Ampulex compressa*; **B.** *Sceliphron destillatorium*. **dT9-2vf a** and **b** – dorsal tergum 9-second valvifer muscle, portion a and b respectively; **vT9-2vf** – ventral T9 second valvifer muscle; **pT9-2vf** – posterior tergum 9-second valvifer muscle.

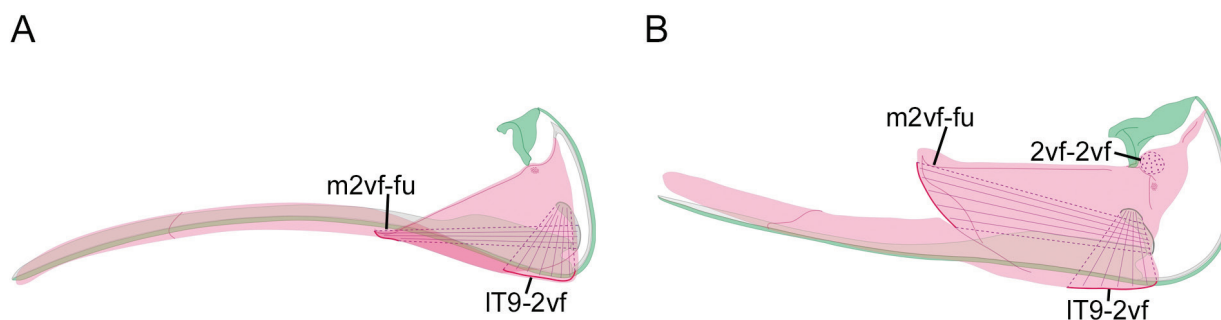


Figure 5. The musculature interconnecting the second valvifer and the furcula. Lateral view, anterior to the right, line drawing from dissections. **A.** *Ampulex compressa*; **B.** *Sceliphron destillatorium*. **l2vf-fu** – lateral second valvifer-furcula muscle; **m2vf-fu** medial second valvifer-furcula muscle; **2vf-2vf** – second valvifer-second valvifer muscle.

Second valvifer to furcula (Fig. 5B)

Second valvifer-second valvifer muscle (2vf-2vf) arises on the dorsal edge of the medial flank of the second valvifer, ventral of the insertion of **dT9-2vf b**, and inserts on the equivalent second valvifer of the opposite body side.

Discussion

The sclerites of the sting apparatus derived from abdominal terga and sterna (Snodgrass 1933, Rietschel 1937). Concealed cuticular segments formed the sclerites T8 and T9 of the sting apparatus. These sclerites are modifications of the respective abdominal tergum 8 and 9. Likewise, the abdominal segment 8 formed the first valvula, first valvifer and first ramus. The abdominal segment 9 formed the second valvifer, second ramus, as well as the second and third valvula (Snodgrass 1933, Trojan 1935, Rietschel 1937, Scudder 1961). All sclerites typically found in the sting apparatus (Matushkina and Stetsun 2016, Kumpanenko and Gladun 2018) were identified in both specimens (Fig. 1). The iodine staining was not intensive enough to distinguish the tiniest sclerotised structures. Therefore, we identified the rami and furcula in *A. compressa* only by dissection.

In comparison with dissected specimens, *S. destillatorium* shows a rotation and ventral shift of the sting apparatus in

the μ CT scan. Comparisons of the stinger and sclerites (Fig. 1B, D) to the illustrations of Kumpanenko and Gladun (2018, fig. 6c) as well as Matushkina (2011, fig. 1A) indicate that our specimen was preserved with a fully extended stinger. In relation to T8, T9 is rotated and shifted anteriorly. The posterior edge of the second valvifer is lifted and the resulting rotation pushes the stinger forward. This results in the sharp angle between second valvifer and third valvula (Fig. 1D). A high density of chemo- and mechanoreceptors on the posterior tip of the third valvula suggests that the posterior third remains on the stinger while being extended, presumably to guide the stinger (Matushkina 2011, Kumpanenko and Gladun 2018). While an extended stinger is of little consequence for the comparison of muscles by origin and insertion, it does allow for an insight into the process of stinging. Nevertheless, the muscles in *S. destillatorium* were described assuming the sclerite position with retracted stinger to maintain comparability.

All four muscles, the **dorsal tergum 7-tergum 8 muscle (dT7-T8)**, the **ventral tergum 7-tergum 8 muscle (vT7-T8)**, the **posterior tergum 7-tergum 8 muscle (pT7-T8)** and the **sternum 7-tergum 8 muscle (S7-T8)**, connecting T8 to T7 and S7, can be found in both examined species (Fig. 2). We propose **dT7-T8** and **S7-T8** to be homologous to Rietschels (1937) muscle 1 and muscle 8, respectively. He described a wide interspecific variety in sclerite and muscle morphology of T8 in *Vespa*, *Prosopis*, *Bombus* and *Apis mellifera* queen and worker. Despite

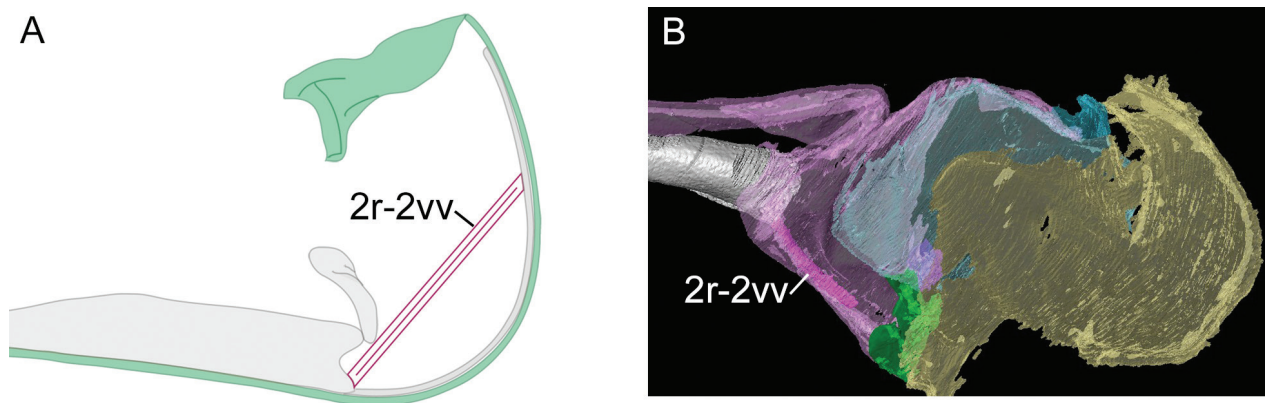


Figure 6. Second ramus-second valvula muscle (2r-2vv) interconnecting the second ramus and second valvula. **A.** Line drawing of 2r-2vv, not found during dissections, based on **B.** reconstructed volume of *Sceliphron destillatorium*. Lateral view, anterior to the right. 2r-2vv – second ramus-second valvula muscle.

this high variability, **dT7-T8** and **S7-T8** were found in all specimens Rietschel (1937) described. The muscles have a similar position, origin and insertion (compare Fig. 2 to Rietschel 1937, figs 7, 9, 11). The **S7-T8** is the only muscle in all described specimens connecting to a sternum. Rietschel (1937) found **dT7-T8** to be bipartite in some species (e.g. of *Bombus* and *Vespa*), but undivided in others (e.g. of *Apis* queen). Neither *S. destillatorium* nor *A. compressa* show a division of **dT7-T8**. As the muscle is rod-like, or at least equally fan-shaped at both sides, we adopted origin and insertion described by Rietschel (1937) for the designation. In *S. destillatorium* **vT7-T8** is bipartite (Fig. 2B). The insertion of **vT7-T8 a** and **b** in *S. destillatorium* and **vT7-T8** in *A. compressa* on the anterior edge of the T8, as well as the origin ventral to **dT7-T8** matches Rietschels (1937) description of his muscle 2. The fourth muscle, **pT7-T8** (Fig. 2A), is homologue to muscle 3 of Rietschel (1937). We were not able to certainly identify this muscle in the μ CT scan of *A. compressa*, as *in situ* the muscles interconnecting the seventh and eighth abdominal segment run close together and are inseparable from the scan. However, **pT7-T8** is large enough to be certainly identified under the binocular. It is the only muscle connecting the T8 to the cuticula that is directed posteriorly and might as such enhance the manoeuvrability of the T8, and thereby the sting apparatus as a whole. All four muscles (**ventral**, **dorsal** and **posterior T7-T8** as well as **S7-T8**) are not described in the HAO.

Muscles described in the HAO and by Vilhelmsen et al. (2001, Orussidae), Vilhelmsen (2000c, basal Hymenoptera) and Ernst et al. (2013, Ceraphronoidea) were studied in species with an ovipositor. The evolution of the ovipositor into the sting apparatus is evident in the high number of homologous muscles explained below. The homologies between the sting apparatus of Chrysididae (Barbosa et al. 2021) and the species described herein can be tracked comparing both to the pompilid *Cryptocheilus versicolor* (Kumpanenko and Gladun 2018). Chrysididae is the sister group to the monophyletic taxon containing Pompilidae and Apoidea, within which Pompilidae occupies a relatively basal position.

The **tergum 8-first valvifer muscle (T8-1vf)** is the only muscle associated with the first valvifer (Fig. 3). It is therefore easy to homologize it with muscle 14 in Rietschel (1937), M4 in Kumpanenko and Gladun (2018) and with the muscle described on the HAO.

The HAO describes the **dorsal tergum 8-tergum 9 muscle (dT8-T9)** (Fig. 3) arising on the anteromedian margin of T8 and inserting on the anteromedian margin of T9. This description may be misleading, because the only way to connect T8 and T9 is, that **dT8-T9** arises from T8, facing the centre of the body (medial), and inserts on the flank of T9, facing the cuticle (lateral). In our case, we described the muscle as originating medially on T8 and inserting laterally on T9. The homology of **dT8-T9** to the described muscle can be deduced from their comparable situation and course (compare Fig. 3 to Ernst et al. 2013, figs 1B, 2A, D), as well as from their insertion.

As the anal arch in *S. destillatorium* is well pronounced, we can clearly identify the insertion of **dT8-T9** on the apodeme of the anal arch (Fig. 3B). In *A. compressa*, with a thin and less sclerotised anal arch, **dT8-T9** appears to insert on the posterodorsal edge of T9, dorsal of the anal arch (Fig. 3A). The lesser sclerotisation might not provide the necessary stability for strong muscles to arise from the anal arch. In return it may allow for the halves of T9 to be moved more independently, enhancing stinger manoeuvrability.

The **dT8-T9** and the **lateral tergum 8-tergum 9 muscles (lT8-T9)** originate close together and run in roughly a perpendicular angle from each other. This muscle group, including **T8-1vf**, can be observed in both of our species (Fig. 3) as well as in those described by Ernst et al. (2013, figs 1B, 2A, D), Kumpanenko and Gladun (2018, fig. 5A, muscle 2 and 3) and Rietschel (1937, figs 9b, 10b, 11b, muscle 10 and 11).

The **tergum 8-tergum 8 muscle (T8-T8)** is the only one interconnecting T8 and was only found in *A. compressa* (Fig. 3A). However, Rietschel (1937) identified two muscles in every specimen illustrated (*Bombus*, *Vespa*, *Prosopis*, *Apis mellifera* queen and worker), which interconnect the T8. As **T8-T8** arises on the ventral rim

of the spiracle, it matches the description of Rietschels (1937) muscle 13. Muscle 12 is supposed to run across the spiracle, which is not the case for **T8-T8**. Kumpanenko and Gladun (2018) neither described any muscles interconnecting the same female tergum, nor did they mention their absence. The HAO does not provide any information on such muscles.

Moreover, the **ventral tergum 8-tergum 9 muscle (vT8-T9)** is only present in *A. compressa* (Fig. 3B). So far, we did not find any information about this muscle in the literature. In contrast to the scanning result, the dissections of *A. compressa* could not verify the existence of **vT8-T9**, which might be due to its small size. On the scan it is clearly identifiable on both body sides.

The **dorsal tergum 9-second valvifer muscle (dT9-2vf) a** and **b** and the **ventral tergum 9-second valvifer muscle (vT9-2vf)** form a group of muscles consistently found in our specimens (Fig. 4). They were also described by Rietschel (1937, muscles 17a/b and 18) and Kumpanenko and Gladun (2018, M5 a/b and 6). Furthermore, this group was described for other specimens with an ovipositor by the HAO, based on Ernst et al. (2013, fig. 4A–F) and Vilhelmsen et al. (2001, fig. 9A). The **dT9-2vf** is always split into two portions which originate on T9 and insert on the articular process of the second valvifer. In *S. destillatorium*, **portion a** and **b** of **dT9-2vf** originate from the anal arch. In *A. compressa* they originate on the lateral and medial flank of T9 respectively. The **vT9-2vf** is supposed to be the antagonist of **dT9-2vf**; the alternating contractions of both muscles extend and retract the first valvula (Rietschel 1937, Vilhelmsen 2000c, Kumpanenko and Gladun 2018). This interplay allows non-aculeate Hymenoptera to drill their ovipositor into the substrate and subsequently transport the egg into the cavity (Vilhelmsen 2000c). In apoid wasps these muscles, through the alternate movement of the first valvulae, pump the venom down the stinger (Kumpanenko and Gladun 2018). In the described position and function, **vT9-2vf** is homologue to Rietschels (1937) muscle 18 and the muscle described in the HAO. Kumpanenko and Gladun (2018) designate their M6 as arising from T9 and inserting on the second valvifer, as described in other literature. Contrarily, their figures (Kumpanenko and Gladun 2018, fig. 5B) show the muscle to be fan-shaped at the connection to the 2vf. Based on the similar situation and expected function, the muscle is homologue to our **vT9-2vf**.

The **posterior T9-second valvifer muscle (pT9-2vf)** was found in both specimens and clearly is homologous to the one described by the HAO, Vilhelmsen (2000b), Ernst et al. (2013), and Kumpanenko and Gladun (2018, M7) (Fig. 4). Due to the weakly sclerotised anal arch in *A. compressa*, we expected **pT9-2vf** to arise posteriorly on the dorsal edge of T9, comparable to **dorsal** and **ventral T9-2vf**, which arise on the dorsal flank of the T9. Instead the origin of **pT9-2vf** is found posteroventral on the anal arch in *A. compressa* (Fig. 4A). We support the assumption of Kumpanenko

and Gladun (2018, on the basis of M7), that the **pT9-2vf** is responsible for transferring the rotation of T9 to the second valvifer.

A muscle connecting the second ramus and the base of the stinger, **second ramus-second valvula muscle (2r-2vv)**, might be missing completely in *A. compressa* and *S. destillatorium*. It would be homologues to M10 of Kumpanenko and Gladun (2018) and to muscle 20 of Rietschel (1937) where it was only attributed a supporting role in stinger retraction. Only in the μ CT scan of *S. destillatorium* indications of such a muscle (Fig. 6A) could be found, but dissections suggest that the reconstructed volume (Fig. 6B) is made up of parts of the rami and surrounding soft tissue. No indication of **2r-2vv** could be found in any dissected specimen.

The **medial second valvifer-furcula muscle (m2vf-fu)** and the **lateral second valvifer-furcula muscle (l2vf-fu)** (Fig. 5) connect the second valvifer to the furcula. Both muscles run very close together in *A. compressa* and were difficult to separate. Hermann and Chao (2002) described, in contrast to Snodgrass (1933), two muscles connecting to the furcula. This was also observed by Rietschel (1937), who described two parts of muscle 19. His description and illustrations of part A matches M9 of Kumpanenko and Gladun (2018) and **m2vf-fu**; part B was described as arising near the articular process. Our observations confirm **l2vf-fu** arising on the ventral edge of the 2vf as described by Kumpanenko and Gladun (2018). The terminology used by Hermann and Chao (2002) appointed **m2vf-fu** as depressor and **l2vf-fu** as rotator of the stinger. The HAO has not listed any muscles interconnecting the second valvifer and the furcula. The **second valvifer-second valvifer muscle (2vf-2vf)** (Fig. 5B) interconnects the second valvifer of both body sides in *S. destillatorium*; it is one continuous, traverse muscle. No comparable muscle was found in *A. compressa*. Vilhelmsen (2000c) described a muscle, the 2vf-genital membrane muscle, arising dorsally on the first valvifer and inserting on the genital membrane, thus close to its counterpart from the other body side. However, we could neither identify a membrane in-between **2vf-2vf** nor any tissue posterior or anterior to the muscle.

Additionally, we found two muscles connecting the sting apparatus to a membrane in both specimens. As they do not fulfil a function in stinger extension, we mention them only for completeness according to the region of interest. One muscle arises near the antero-medial edge of the T8, the second one arises postero-dorsally on the medial flank of T9 below the anal arch. The muscles insert on different round membranes, positioned centrally in between the sclerites of the sting apparatus. Most likely these are the gut and venom bladder. Possibly the one arising from the T9 is homologue to the T9-genital membrane muscle identified by Vilhelmsen (2000c). The presence of the muscles originating from T9 in *A. compressa* and the presence of the muscle originating from the T8 in *S. destilla-*

torium could be verified during dissections. The additional connections to the membranes might also be non-muscular tissue. Their presence would contradict the hypothesis of Barbosa et al. (2021), that the loss of muscles connecting to the genital membrane is an autapomorphy of Aculeata.

On the physiological act of stinging

Snodgrass (1933) and Rietschel (1937) showed that rising pressure in the metasoma is not responsible for the extension of the stinger. Based on Snodgrass (1933), Rietschel (1937) proposed **m2vf-fu** to be responsible for the extension. Abdominal sternum 7 supposedly works as a counter bearing to convert the downward movement of the stinger induced by **m2vf-fu** into a backward movement. Snodgrass (1933) remarked that the extension of the stinger is accompanied by a dorsal and anterior shift of the whole sting apparatus. But Rietschel (1937) entirely dismissed the proposition of Trojan (1935) that the extension of the stinger is caused by the musculature associated to T8 and T9. He discarded the explanation as too complex and the muscles as too weak to allow this movement. Kumpanenko and Gladun (2018) strongly suggested that the musculature of T8 and T9 indeed rotate T9 for extending the stinger. This rotation is supported by **m2vf-fu**, pushing the stinger farther posterior to pierce the integument of the prey (Kumpanenko and Gladun 2018).

Like Barbosa et al. (2021) in Chrysoidea, we found several indications supporting the theory of Kumpanenko and Gladun (2018). The main evidence is the anterodorsal rotation of T9 and second valvifer. This rotation results in the ventral shift of the first valvifer, connecting the second valvifer and T9 (Fig. 1B, D). The **dT8-T9** and **T8-1vf** most likely rotate T9, as described by Kumpanenko and Gladun (2018). It is difficult to assess whether **vT8-T9**, only present in *A. compressa*, supports the rotation of T9. Together with **IT8-T9** it might as well act as additional antagonist to **dT8-T9** and **T8-1vf**.

The rotation of T9 is transferred to the second valvifer via the elastic rami. Further rotation is provided by **pT9-2vf**, which was found in both specimens, opposed to Rietschel (1937), who did not find this muscle. The insertion of **m2vf-fu** in *S. destillatorium* with extended stinger (Fig. 1D) is found farther posterodorsal compared to the insertion in *A. compressa* (Fig. 1C), where it is located medial to **l2vf-fu**. This indicates that the furcula is rotated by **m2vf-fu**; the dorsal arm is now pulled posterodorsally, leveraging the force of **l2vf-fu** to maximally extend the stinger. This is in line with the anterior and posterior second valvifer-second valvula muscles (Vilhelmsen 2000c), homologue to lateral and medial **2vf-fu** muscles, serving as rotators to extend the first and second valvulae from in-between the ovipositor sheaths in non-aculeate Hymenoptera. The flexible rami act as antagonists of the **lateral** and **dorsal 2vf-fu**.

Conclusion

We provided descriptions and illustrations allowing for the comparison of the musculature of the sting apparatus *in situ*. We showed that this musculature is almost identical among *A. compressa* and *S. destillatorium*. The high number of identified homologies of our species with those described in other literature suggests that our collective understanding of the basal musculature continues to increase. See Suppl. material 2: Table S2 for a homologisation of the terminology used by different authors. As this is the first detailed study on the musculature of the sting apparatus in digger wasps, further research is needed to identify muscles of phylogenetic significance. Rietschel (1937) apparently dissected *Ammophila* and *Cerceris*, but did not specify which muscles beside **S7-T8** he found. In addition to contemporary functional analyses of the sting apparatus, morphological studies should also deal with the musculature connecting to the cuticle, as it bears significant interspecific differences in the available literature (Snodgrass 1933, Rietschel 1937). Rietschel's (1937) suggestion that the presence of **dorsal, ventral and posterior T7-T8** is the plesiomorphic condition, seems to be supported by the presence of all three muscles in *A. compressa* and *S. destillatorium*.

Acknowledgements

We would like to thank Anke Sanger, Kristin Mahlow and Prof. Dr Johannes Muller for the constant technical support. Many thanks to the Zuse Institute Berlin, especially Dr Daniel Baum, for providing AmiraZIB, and to the Aqua Zoo Dusseldorf, especially Sandra Honigs and Dieter Schulten, for fresh *Ampulex compressa* specimens. Furthermore, we thank Dr Austin Alleman for proofreading. We gratefully acknowledge the coverage of publication costs by the Museum fur Naturkunde Berlin.

References

- Aguiar AP, Deans AR, Engel MS, Forshage M, Huber JT, Jennings JT, Johnson NF, Lelej AS, Longino JT, Lohrmann V, Miko I, Ohl M, Rasmussen C, Taeger A, Sick Ki Yu D (2013) Order Hymenoptera. In: Zhang ZQ (Ed.) Animal biodiversity: an outline of higher-level classification and survey of taxonomic richness (addenda 2013). Zootaxa 3703: 51–62. <https://doi.org/10.11646/zootaxa.3703.1.12>
- Barbosa DN, Vilhelmsen L, Azevedo CO (2021) Morphology of sting apparatus of Chrysoidea (Hymenoptera, Aculeata). Arthropod Structure & Development 60: 100999. <https://doi.org/10.1016/j.asd.2020.100999>
- Bohart RM, Menke AS (1976) Sphecid wasps of the World: A generic revision. University of California Press, Berkeley, 694 pp. https://archive.org/details/bub_gb_FExMjuRhjIC/page/n27
- Branstetter MG, Danforth BN, Pitts JP, Gates MW, Kula RR, Brady G, Branstetter MG, Danforth BN, Pitts JP, Faircloth BC, Ward PS (2017) Phylogenomic insights into the evolution of stinging wasps and the origins of ants and bees. Current Biology 27(7): 1019–1025. <https://doi.org/10.1016/j.cub.2017.03.027>

- Catania KC (2018) How not to be turned into a zombie. *Brain, Behavior and Evolution* 92 (32): 32–46. <https://doi.org/10.1159/000490341>
- Ernst AF, Mikó I, Deans AR (2013) Morphology and function of the ovipositor mechanism in Ceraphronoidea (Hymenoptera, Apo-crita). *Journal of Hymenoptera Research* 33: 25–61. <https://doi.org/10.3897/jhr.33.5204>
- Evans HE (1962) The evolution of prey-carrying mechanisms in wasps. *Evolution* 16(4): 468–483. <https://doi.org/10.1111/j.1558-5646.1962.tb03237.x>
- Fateryga AV, Kovblyuk MM (2014) Nesting ecology of the wasp *Sceliphron destillatorium* (Illiger, 1807) (Hymenoptera, Sphecidae) in the Crimea. *Entomological Review* 94(3): 330–336. <https://doi.org/10.1134/S001387381403004X>
- Gadallah NS, Assery BM (2015) Comparative study of the sting apparatus of some Sphecidae collected from Jeddah (west of Saudi Arabia). *Linzer biologische Beiträge* 36(2): 1393–1412.
- Gignac PM, Kley NJ, Clarke JA, Colbert MW, Morhardt AC, Cerio D, Cost IN, Cox PG, Daza JD, Early CM, Echols MS, Henkelman RM, Herdina AN, Holliday CM, Li Z, Mahlow K, Merchant S, Müller J, Orsbon CP, Paluh DJ, Thies ML, Tsai HP, Witmer LM (2016) Diffusible iodine-based contrast-enhanced computed tomography (diceCT): An emerging tool for rapid, high-resolution, 3D imaging of metazoan soft tissues. *Journal of Anatomy* 228(6): 889–909. <https://doi.org/10.1111/joa.12449>
- Grimaldi D, Engel MS (2005) *Evolution of the Insects*. Camarch University Press, Camarch, 429 pp.
- Haspel G, Rosenberg LA, Libersat F (2003) Direct injection of venom by a predatory wasp into cockroach brain. *Journal of Neurobiology* 56(3): 287–292. <https://doi.org/10.1002/neu.10238>
- Hermann HR, Chao J (2002) Furcula, a major component of the hymenopterous venom apparatus. *International Journal of Insect Morphology and Embryology* 12(5): 1–17. [https://doi.org/10.1016/0020-7322\(83\)90027-2](https://doi.org/10.1016/0020-7322(83)90027-2)
- Hymenoptera Anatomy Consortium (2020) Hymenoptera Anatomy Consortium. <http://glossary.hymao.org>
- Kugler C (1978) A comparative study of the myrmicine sting apparatus (Hymenoptera, Formicidae). *Studia Entomologica* 20: 413–548.
- Kumpanenko AS, Gladun DV (2018) Functional morphology of the sting apparatus of the spider wasp *Cryptocheilus versicolor* (Scopoli, 1763) (Hymenoptera: Pompilidae). *Entomological Science* 21(1): 124–132. <https://doi.org/10.1111/ens.12288>
- Libersat F (2003) Wasp uses venom cocktail to manipulate the behavior of its cockroach prey. *Journal of Comparative Physiology A* 189: 497–508. <https://doi.org/10.1007/s00359-003-0432-0>
- Liu S, Richter A, Stoessel A, Beutel RG (2019) The mesosomal anatomy of *Myrmecia nigrocincta* workers and evolutionary transformations in Formicidae (Hymenoptera). *Athropod Systematics & Phylogeny* 77(1): 1–19.
- Lohrmann V, Ohl M, Bleidorn C, Podsiadlowski L (2008) Phylogenie der „Sphecidae“ (Hymenoptera: Apoidea) basierend auf molekularen Daten. *Mitteilungen der Deutschen Gesellschaft für allgemeine und angewandte Entomologie* 16: 99–102.
- Matushkina N (2011) Sting microsculpture in the digger wasp *Bembix rostrata* (Hymenoptera, Crabronidae). *Journal of Hymenoptera Research* 21: 41–52. <https://doi.org/10.3897/jhr.21.873>
- Matushkina N, Stetsun HA (2016) Morphology of the sting apparatus of the digger wasp *Oxybelus uniglumis* (Linnaeus, 1758) (Hymenoptera, Crabronidae), with emphasis on intraspecific variability and behavioural plasticity. *Journal of Systematics and Evolution* 47(4): 347–362. <https://doi.org/10.1163/1876312X-47032146>
- Metscher BD (2009) MicroCT for comparative morphology: simple staining methods allow high-contrast 3D imaging of diverse non-mineralized animal tissues. *BMC Physiology* 9: e11. <https://doi.org/10.1186/1472-6793-9-11>
- Mikó I, Vilhelmsen L, Johnson NF, Masner L, Péntzes Z (2007) Skelettomusculature of Scelionidae (Hymenoptera: Platygastridae): head and mesosoma. *Zootaxa* 1571: 1–78. <https://doi.org/10.11646/zootaxa.1571.1.1>
- Mosel S (2014) *Der Stachelapparat aculeater Hymenopteren: Morphologie, Evolution und die Bedeutung für Reproduktionsstrategien bei solitären Wespen*. Ph.D. Dissertation. Humboldt-Universität zu Berlin, Berlin, 100 pp.
- Ohl M, Bleidorn C (2006) The phylogenetic position of the enigmatic wasp family Heterogynaidae based on molecular data, with description of a new, nocturnal species (Hymenoptera: Apoidea). *Systematic Entomology* 31(2): 321–337. <https://doi.org/10.1111/j.1365-3113.2005.00313.x>
- Ohl M, Engel MS (2007) Die Fossilgeschichte der Bienen und ihrer nächsten Verwandten (Hymenoptera: Apoidea). *Denisia* 20(66): 687–700. https://www.zobodat.at/pdf/DENISIA_0020_0687-0700.pdf
- Ohl M, Spahn P (2010) A cladistic analysis of the cockroach wasps based on morphological data (Hymenoptera: Ampulicidae). *Cladistics* 26(1): 49–61. <https://doi.org/10.1111/j.1096-0031.2009.00275.x>
- Packer L (2003) Comparative morphology of the skeletal parts of the sting apparatus of bees (Hymenoptera: Apoidea). *Zoological Journal of the Linnean Society* 138(1): 1–38. <https://doi.org/10.1046/j.1096-3642.2003.00055.x>
- Peters RS, Krogmann L, Mayer C, Donath A, Gunkel S, Meusemann K, Kozlov A, Podsiadlowski L, Petersen M, Lanfear R, Diez PA, Heraty J, Kjer KM, Klopstein S, Meier R, Polidori C, Schmitt T, Liu S, Zhou X, Wappler T, Rust J, Misof B, Niehuis O (2017) Evolutionary history of the Hymenoptera. *Current Biology* 27(7): 1013–1018. <https://doi.org/10.1016/j.cub.2017.01.027>
- Pulawski WJ (2020) Catalog of Sphecidae sensu lato (= Apoidea excluding Apidae). <http://www.calacademy.org/scientists/projects/catalog-of-sphecidae>
- Rietschel P (1937) Bau und Funktion des Wehrstachels der Staatenbildenden Bienen und Wespen. *Zeitschrift für Morphologie und Ökologie der Tiere* 33: 313–357. <https://doi.org/10.1007/BF00407850>
- Sann M, Niehuis O, Peters RS, Mayer C, Kozlov A, Podsiadlowski L, Bank S, Meusemann K, Misof B, Bleidorn C, Ohl M (2018) Phylogenomic analysis of Apoidea sheds new light on the sister group of bees. *BMC Evolutionary Biology* 18(71): 1–15. <https://doi.org/10.1186/s12862-018-1155-8>
- Scudder GGE (1961) The functional morphology and interpretation of the insect ovipositor. *The Canadian Entomologist* 93(4): 267–272. <https://doi.org/10.4039/Ent93267-4>
- Sharkey MJ, Carpenter JM, Vilhelmsen L, Heraty J, Dowling APG, Schulmeister S, Murray D, Andrew R, Ronquist F, Krogmann L, Wheeler WC (2012) Cladistics phylogenetic relationships among superfamilies of Hymenoptera. *Cladistics* 28: 80–112. <https://doi.org/10.1111/j.1096-0031.2011.00366.x>
- Da Silva M, Noll FB, Carpenter JM (2014) The usefulness of the sting apparatus in phylogenetic reconstructions in vespids, with emphasis on the Epiponini: More support for the single origin of eusociality in the Vespidae. *Neotropical entomology* 43: 134–142. <https://doi.org/10.1007/s13744-013-0179-4>

- Smith EL (1970) Evolutionary morphology of the external insect genitalia. 2. Hymenoptera. *Annals of the Entomological Society of America* 63(1): 1–27. <https://doi.org/10.1093/aesa/63.1.1>
- Snodgrass RE (1933) How the bee stings. *Bee World* 14(1): 3–6. <https://doi.org/10.1080/0005772X.1933.11093188>
- Trojan E (1935) Zur Frage der Oligomerie Weiblicher Akuleaten. *Zeitschrift für Morphologie und Ökologie der Tiere* 30(4): 597–628. <https://doi.org/10.1007/BF00403139>
- Vilhelmsen L (2000a) Before the wasp-waist: Comparative anatomy and phylogenetic implications of the skeleto-musculature of the thoraco-abdominal boundary region in basal Hymenoptera. *Zoomorphology* 119: 185–221. <https://doi.org/10.1007/PL00008493>
- Vilhelmsen L (2000b) Cervical and prothoracic skeleto-musculature in the basal Hymenoptera (Insecta): comparative anatomy and phylogenetic implications. *Zoologischer Anzeiger* 239(2): 105–138.
- Vilhelmsen L (2000c) The ovipositor apparatus of basal Hymenoptera (Insecta): phylogenetic implications and functional morphology. *Zoologica Scripta* 29(4): 319–345. <https://doi.org/10.1046/j.1463-6409.2000.00046.x>
- Vilhelmsen L, Isidoro N, Romani R, Basibuyuk HH, Quicke DLJ (2001) Host location and oviposition in a basal group of parasitic wasps: the subgenual organ, ovipositor apparatus and associated structures in the Orussidae (Hymenoptera, Insecta). *Zoomorphology* 121: 63–84. <https://doi.org/10.1007/s004350100046>
- Vilhelmsen L, Miko I, Krogmann L (2010) Beyond the wasp-waist: structural diversity and phylogenetic significance of the mesosoma in apocritan wasps (Insecta: Hymenoptera). *Zoological Journal of the Linnean Society* 159(1): 22–194. <https://doi.org/10.1111/j.1096-3642.2009.00576.x>
- Willsch M, Friedrich F, Baum D, Jurisch I, Ohl M (2020) A comparative description of the mesosomal musculature in Sphecidae and Ampulicidae (Hymenoptera, Apoidea) using 3D techniques. *Deutsche Entomologische Zeitschrift* 67(1): 51–67. <https://doi.org/10.3897/dez.67.49493>
- Yoder M, Mikó I, Seltmann K, Bertone M, Deans A (2010) Hymenoptera Anatomy Ontology Portal. *PLoS ONE* 5(12): e15991. <https://doi.org/10.1371/journal.pone.0015991>
- Zimmermann D, Vilhelmsen L (2016) The sister group of Aculeata (Hymenoptera) – evidence from internal head anatomy, with emphasis on the tentorium. *Athropod Systematics & Phylogeny* 74(2): 195–218. https://curis.ku.dk/portal/files/171586094/05_asp_74_2_zimmermann_195_218.pdf

Supplementary material 1

Table S1. Detailed list of specimens and their collection/rearing data

Authors: Stefan Graf, Maraike Willsch, Michael Ohl

Data type: specimens, label data

Explanation note: Detailed list of specimens including MfN collection ID and all available label data.

Copyright notice: This dataset is made available under the Open Database License (<http://opendatacommons.org/licenses/odbl/1.0>). The Open Database License (ODbL) is a license agreement intended to allow users to freely share, modify, and use this Dataset while maintaining this same freedom for others, provided that the original source and author(s) are credited.

Link: <https://doi.org/10.3897/dez.68.58217.suppl1>

Supplementary material 2

Table S2. Overview of all muscles with HAO URIs and the proposed homologies

Authors: Stefan Graf, Maraike Willsch, Michael Ohl

Data type: morphological, homologies, URIs

Explanation note: All described muscles with additional HAO Universal Resource Identifiers (URI) and the proposed homologies with Rietschel (1937) and Kumpanenko and Gladun (2018).

Copyright notice: This dataset is made available under the Open Database License (<http://opendatacommons.org/licenses/odbl/1.0>). The Open Database License (ODbL) is a license agreement intended to allow users to freely share, modify, and use this Dataset while maintaining this same freedom for others, provided that the original source and author(s) are credited.

Link: <https://doi.org/10.3897/dez.68.58217.suppl2>